Supplementary Material for

Production of methyl vinyl ketone and methacrolein via the hydroperoxyl pathway of isoprene oxidation

by

Y. J. Liu (1), I. Herdlinger-Blatt (1,2), K. A. McKinney* (3), and S.T. Martin* (1,4)

(1) School of Engineering and Applied Sciences, Harvard University, Cambridge, Massachusetts, USA

(2) Institute of Ion Physics and Applied Physics, University of Innsbruck, Innsbruck, Austria

(3) Department of Chemistry, Amherst College, Amherst, Massachusetts, USA

(4) Department of Earth and Planetary Sciences, Harvard University, Cambridge, Massachusetts, USA

E-mail: kamckinney@amherst.edu

scot_martin@harvard.edu

http://www.seas.harvard.edu/environmental-chemistry

*To Whom Correspondence Should be Addressed

A. Calibration of NO_x analyzer

The instrument background in the absence of NO was obtained by converting NO to NO_2 in the dry air from the pure air generator with additional ozone immediately before the NO detector. The instrument sensitivity of NO was obtained by repeated calibration with NO standard diluted with dry air and the instrumental sensitivity of NO_2 was obtained by converting NO to NO_2 with additional ozone. The signals of NO and NO_x of the dry air from pure air generator had no significant difference from instrument background.

B. PTR-TOF-MS data analysis routine

(1) Peak shape fitting

A numerical peak shape was generated for each 6-min sum spectrum as described in the main text. No significant change of peak shape was observed within any one HDF file we have collected, which was usually for less than 12 hr. Therefore, an averaged numeric peak shape was used for each signal HDF file. The shape-fitting peaks used for the NO^+ mode include H_3O^+ (*m/z* = 19.0178 Th), NO_2^+(*m/z* = 45.9924 Th) and $C_5H_8^+$ (*m/z* = 68.0621 Th, only for chamber steady-state conditions). For the H_3O^+ mode, $H_3{}^{18}O^+$ (*m/z* = 21.0221 Th), NO^+(*m/z* = 29.9974 Th) and $H_5O^{18}O^+$ (*m/z* = 39.0327 Th) were used.

(2) Mass calibration

Using a generated peak shape, a peak fitting algorithm was then applied to a list of mass calibration peaks to optimize the time-of-flight of their peak maximum. In the case of NO^+ mode, the mass calibration peaks included H_3O^+, NO_2^+, $H_2NO_2^+$ (*m/z* = 48.0080 Th), and $C_5H_8^+$ (only for chamber steady-state conditions). For H_3O^+ mode, the mass calibration peaks included H_3O^{18+}, NO^+, $H_5O^{18}O^+$, NO_2^+ (*m/z* = 45.9924 Th) and $H_7O_3^+$ (*m/z* = 55.0390 Th). The

relationship of the time-of-light and the mass-to-charge ratio (*m*/*z*) was calculated according to the following equation by fitting the coefficients α and β:

$$m/z = \left(\frac{\mathrm{TOF} - \beta}{\alpha}\right)$$

The mass calibration peaks covered only the *m/z* range below 70 Th, but the *m*/*z* of the ions generated from isoprene oxidation products were expected to be as high as 120 Th. To examine whether this could be a source of inaccuracy for mass calibration, an external mass calibration compound, 1,4-dicholorobenzene, was added. The product ions of 1,4-dicholobenzene $C_6H_4Cl_2^+$ (*m/z* = 145.968) and $C_6H_4Cl_2NO^+$ (*m/z* = 175.966) were used for the mass calibration at the NO^+ mode. For the H_3O^+ mode, $C_6H_5Cl_2^+$ (*m/z* = 146.976) was used. The deviation of the mass calibration curve obtained with and without 1,4-dicholorobenzene ions was below 5 ppm for both modes in the m/z range below 150 Th. Therefore, the mass calibration without adding external calibration compound worked well for the interested mass range.

(3) Peak assignment

With a good mass calibration and a well-defined peak shape, we then assigned ion formula for the peaks in the full *m/z* range. A pre-existing ion list was created, containing all possible combination of C, H, O, N, and their important isotopes for *m/z* < 200 Th. A target peak was first fitted using the ion with an *m/z* ratio most close to the peak maximum. If there was a significant residual peak left, a second ion with an *m/z* ratio most close to the residual peak maximum was added into the fitting procedure. The peak assignment process was done manually to avoid missing any shoulder peaks.

(4) Signal analysis

For signal analysis, peak fitting algorithm was applied on the target peaks using pre-assigned ion formulas. The resulting peak signal (cps) were normalized to a primary ion signal of 10^6 cps without transmission correction (cps → ncps), as described by de Gouw et al. (2003)

C. Wall-loss experiment

Separate chamber experiments were performed to test the wall loss of isoprene, MVK and MACR. The target species were continuously injected into the chamber bag using syringe pump until their concentrations got stabilized. Inflows and injection were then stopped for 2 hr. At the same time the gas-phase concentrations of the target species were continuously measured. No drop in the signal of ISOP, MVK, and MACR was observed, suggesting negligible wall loss at steady state.

D. Dependence of the sensitivities on the E/N ratio

The influence of electric field (*E*/*N* ratio) on the sensitivity response of ISOP, MVK, and MACR for the NO^+ mode is illustrated in Figure S3. The sensitivities of the three compounds decreased for increasing *E*/*N*. The ratio of $C_4H_6O{\cdot}NO^+/C_4H_5O^+$ ion signals for MACR also decreased for increasing *E*/*N*. To ensure better separation of MACR from MVK which only produced $C_4H_6O{\cdot}NO^+$ ions and at the same time high sensitivities for both species, the drift tube voltage was kept at 300 V and drift tube temperature at 60 ℃ during chamber experiments, corresponding to an *E*/*N* ratio of 68 Td.

As shown in Figure S3, at lower *E*/*N* ratios smaller changes in the sensitivity of isoprene were observed. A similar trend was also observed by Knighton et al. (2009) and Karl et al.

(2012). As a comparison point, the sensitivity in the present work of isoprene was 14.6 ncps ppb^{-1} for an *E*/*N* ratio of 104 Td. This sensitivity is close to the value of 12.5 ncps ppb^{-1} obtained by Karl et al. using a similar PTR-TOF-MS instrument estimated from Figure 3 in that paper. This value is, however, significantly lower than that of 21 ncps ppb^{-1} obtained by Knighton et al. using a PTR-QMS instrument, as estimated from Figure 4 in that paper.

E. Equations for concentration quantification

Concentrations of ISOP, MVK, and MACR in the chamber outflow were quantified using the following equations:

$$[\text{Isoprene}] = \frac{i[C_5H_8^+] - i[C_5H_8^+]_{bg}}{s[C_5H_8^+, \text{Isoprene}]} \quad \text{(S1)}$$

$$[\text{MACR}] = \frac{i[C_4H_5O^+] - i[C_4H_5O^+]_{bg} - 0.011\,(i[C_5H_8] - i[C_5H_8]_{bg})}{s[C_4H_5O^+, \text{MACR}]} \quad \text{(S2)}$$

$$[\text{MVK}] = \frac{i[C_4H_6O\cdot NO^+] - i[C_4H_5O^+]_{bg} - s[C_4H_6O\cdot NO^+, \text{MACR}]\, c[\text{MACR}]}{s[C_4H_6O\cdot NO^+, \text{MVK}]} \quad \text{(S3)}$$

where [M] was the concentration of species M in the chamber air, $i[N^+]$ (cps) was the measured signal of ion N^+ for chamber air, $i[N^+]_{bg}$ (cps) was the measured background signal of ion N^+ using zero air, and $s[N^+,M]$ (cps ppb^{-1}) was the sensitivity of compound M with respect to ion N^+, as determined by calibration. A small amount of $C_4H_5O^+$ was also produced from isoprene (1.1% of $C_5H_8^+$ ion), which was taken into account in converting ion signals to concentrations.

F. Equation for yield determination with ozone correction

$$0 = \left(Y_{MVK}\, k_{\mathrm{ISOP+OH}}\,[\mathrm{OH}]_{ss}[\mathrm{ISOP}]_{ss} + Y_{MVK,O_3}\, k_{\mathrm{ISOP+O_3}}\,[\mathrm{O_3}]_{ss}[\mathrm{ISOP}]_{ss}\right)_{sources} - \left(\begin{array}{l} k_{\mathrm{MVK+OH}}\,[\mathrm{OH}]_{ss}\,[\mathrm{MVK}]_{ss} + k_{\mathrm{MVK+O_3}}\,[\mathrm{O_3}]_{ss}\,[\mathrm{MVK}]_{ss} \\ + \dfrac{1}{\tau}[\mathrm{MVK}]_{ss} + k_{wall}\,[\mathrm{MVK}]_{ss} \end{array}\right)_{sinks} \quad \text{(S4)}$$

$$Y_{MVK} = \frac{(k_{\mathrm{MVK+OH}}\,[\mathrm{OH}]_{ss} + k_{\mathrm{MVK+O_3}}\,[\mathrm{O_3}]_{ss} + 1/\tau + k_{wall})[\mathrm{MVK}]_{ss}}{k_{\mathrm{ISOP+OH}}\,[\mathrm{OH}]_{ss}\,[\mathrm{ISOP}]_{ss}} - \frac{Y_{\mathrm{MVK,O_3}}\, k_{\mathrm{ISOP+O_3}}\,[\mathrm{O_3}]_{ss}[\mathrm{ISOP}]_{ss}}{k_{\mathrm{ISOP+OH}}\,[\mathrm{OH}]_{ss}\,[\mathrm{ISOP}]_{ss}} \quad \text{(S5)}$$

$$0 = \left(\frac{1}{\tau}[\mathrm{ISOP}]_{in}\right)_{sources} - \left(k_{\mathrm{ISOP+OH}}\,[\mathrm{OH}]_{ss}\,[\mathrm{ISOP}]_{ss} + k_{\mathrm{ISOP+O_3}}\,[\mathrm{O_3}]_{ss}\,[\mathrm{ISOP}]_{ss} + \frac{1}{\tau}[\mathrm{ISOP}]_{ss}\right)_{sinks} \quad \text{(S6)}$$

where $k_{\mathrm{ISOP+O3}}$ and $k_{\mathrm{MVK+O3}}$ are the reaction rate coefficients of ISOP and MVK with O_3 and $Y_{\mathrm{MVK,O3}}$ is the yield of MVK from ozonolysis of isoprene.

H. Dependence of the interference on instrumental conditions

To understand whether thermal decomposition of the condensing compounds, possibly ISOPOOH, occurred in the instrument (60 ℃), the change in ion signals of steady-state chamber air was monitored at a low drift tube temperature of 30 ℃ as the inlet temperature was varied from 30 ℃ to 80 ℃. The trap temperature was kept at 25 ℃. The residence times of the sample air in the drift tube and in the inlet line were about the same (60-80 ms). No significant change in ion signals was observed, suggesting that thermal decomposition of other oxidation products inside the instrument did not contribute to the ions at the same *m/z* ratio as MVK and MACR product ions.

Measurements of steady-state chamber air were made at various *E*/*N* ratios in both the NO^+ and H_3O^+ modes. The apparent concentrations of ISOP, MVK, and MACR were quantified with respective calibrations at each *E*/*N* ratio. Here the apparent concentrations are defined as the equivalent concentrations of ISOP, MVK, and MACR assuming no interference compounds. As shown in the top panels of Figure S10, the apparent MVK and MACR concentrations were independent of the *E*/*N* ratio in the range of 15-70 Td in the NO^+ mode and 20-120 Td in the H_3O^+ mode. This observation indicates that the fragmentation of the interference compounds was not sensitive to the collision energies used.

As shown in the bottom panels of Figure S10, the apparent concentrations of MVK and MACR decreased somewhat as the temperature of the drift tube decreased. The apparent concentrations were quantified using respective calibrations at each temperature. The decrease of the apparent concentration of MVK + MACR in NO^+ mode was greater than that of the H_3O^+ mode. This observation suggests that the fragmentation of the condensing compounds was thermally driven, which at first seems inconsistent with the independence of the *E*/*N* ratio. Further investigation is hence needed to fully understand the mechanism.

Reference

de Gouw, J., Warneke, C., Karl, T., Eerdekens, G., van der Veen, C., and Fall, R.: Sensitivity and specificity of atmospheric trace gas detection by proton-transfer-reaction mass spectrometry, Int. J. Mass. Spectrom., 223-224, 365-382, doi: 10.1016/s1387-3806(02)00926-0, 2003.

Karl, T., Hansel, A., Cappellin, L., Kaser, L., Herdlinger-Blatt, I., and Jud, W.: Selective measurements of isoprene and 2-methyl-3-buten-2-ol based on NO^+ ionization mass spectrometry, Atmos. Chem. Phys., 12, 11877-11884, doi: 10.5194/acp-12-11877-2012, 2012.

Knighton, W. B., Fortner, E. C., Herndon, S. C., Wood, E. C., and Miake-Lye, R. C.: Adaptation of a proton transfer reaction mass spectrometer instrument to employ NO^+ as reagent ion for the detection of 1,3-butadiene in the ambient atmosphere, Rapid. Commun. Mass. Sp., 23, 3301-3308, doi: 10.1002/rcm.4249, 2009.

Table S1. Uncertainty Analysis of MVK and MACR yield in Experiment #1 [1]

Input Variables [2]						Output Variables [2]	
Concentrations (ppb) [3]		Reaction rate coefficient, k (molecule^{-1} cm^3 s^{-1}) [4]		Others		Yield (%)	
$[C_5H_8]_{in}$	59.3 ± 2.4	$\log_{10}(k_{C_5H_8+OH})$	-10.00 ± 0.06	τ (hr) [5]	3.7 ± 0.2	MACR	3.2 ± 0.6
$[C_5H_8]_{ss}$	16.0 ± 0.6	$\log_{10}(k_{MACR+OH})$	-10.54 ± 0.10	k_{wall} (s^{-1}) [6]	0	MVK	4.6 ± 0.7
$[MACR]_{ss}$	0.79 ± 0.10	$\log_{10}(k_{MVK+OH})$	-10.70 ± 0.10				
$[MVK]_{ss}$	1.29 ± 0.14						

[1] A Monte Carol method was used for error analysis. All the input variables in Equation 2-3 were taken into consideration (cf. Equation 1-3 for the definitions of the input variables).

[2] (Mean $\pm 2 \times$ Standard Deviation) for all the input and output values.

[3] Uncertainties in concentrations were determined by calibrations.

[4] Reaction rate coefficients and their uncertainties were from IUPAC recommendation in common logarithm.

[5] A 6% 2σ-uncertainty was used for the chamber residence time based on the standard deviation in measured residence times for multiple experiments.

[6] A value of $k_{wall} = 0$ s^{-1} was used based on the results of wall-loss experiments (cf. supplementary material).

List of Figures

40 ℃ in discrete steps. Left column shows the time series of temperature (top) and of ion signals (bottom) in Experiment #1 under HO_2-dominant conditions, and right column shows results for Experiment #7 under NO-dominant conditions. Solid line and dashed line in the bottom panels represent the ion signal of $C_5H_9^+$ and $C_4H_7O^+$, respectively.

Figure S9. Change in the equivalent concentrations of the interference compounds to MVK and MACR with chamber residence time. The equivalent concentration of MVK/MACR interferences is defined as the difference of MVK/MACR concentration at the trap temperature of +25 ℃ and that at -40 ℃. The residence time of reference experiment was 3.7 hr.

Figure S10. Change in the apparent concentrations of isoprene, MVK, and MACR at steady state with the E/N ratios (top) and the drift-tube temperature (bottom) in both NO^+ (left) and H_3O^+ (right) mode. For the H_3O^+ mode, the combined concentration of MVK and MACR was calculated using the average sensitivity of MVK and MACR. The trap temperature was kept at +25 ℃. For the experiments at various E/N ratios, the drift tube temperature was kept on 70 ℃ and the drift tube voltage was varied. For the experiments at various temperatures of the drift tube, the drift tube voltage was 300 V and 520 V for the NO^+ and H_3O^+ modes, respectively.

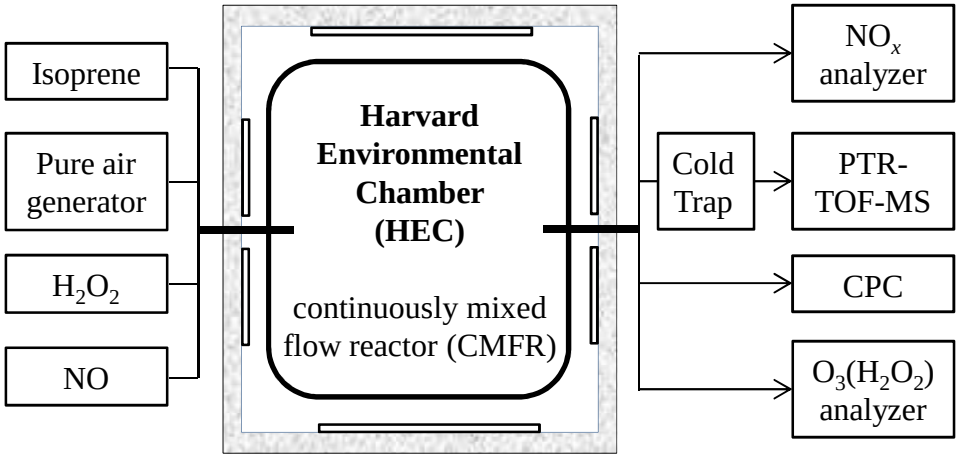
Isoprene
Pure air generator
H_2O_2
NO
Harvard Environmental Chamber (HEC)
continuously mixed flow reactor (CMFR)
Cold Trap
NO_x analyzer
PTR-TOF-MS
CPC
$O_3(H_2O_2)$ analyzer

Figure S1

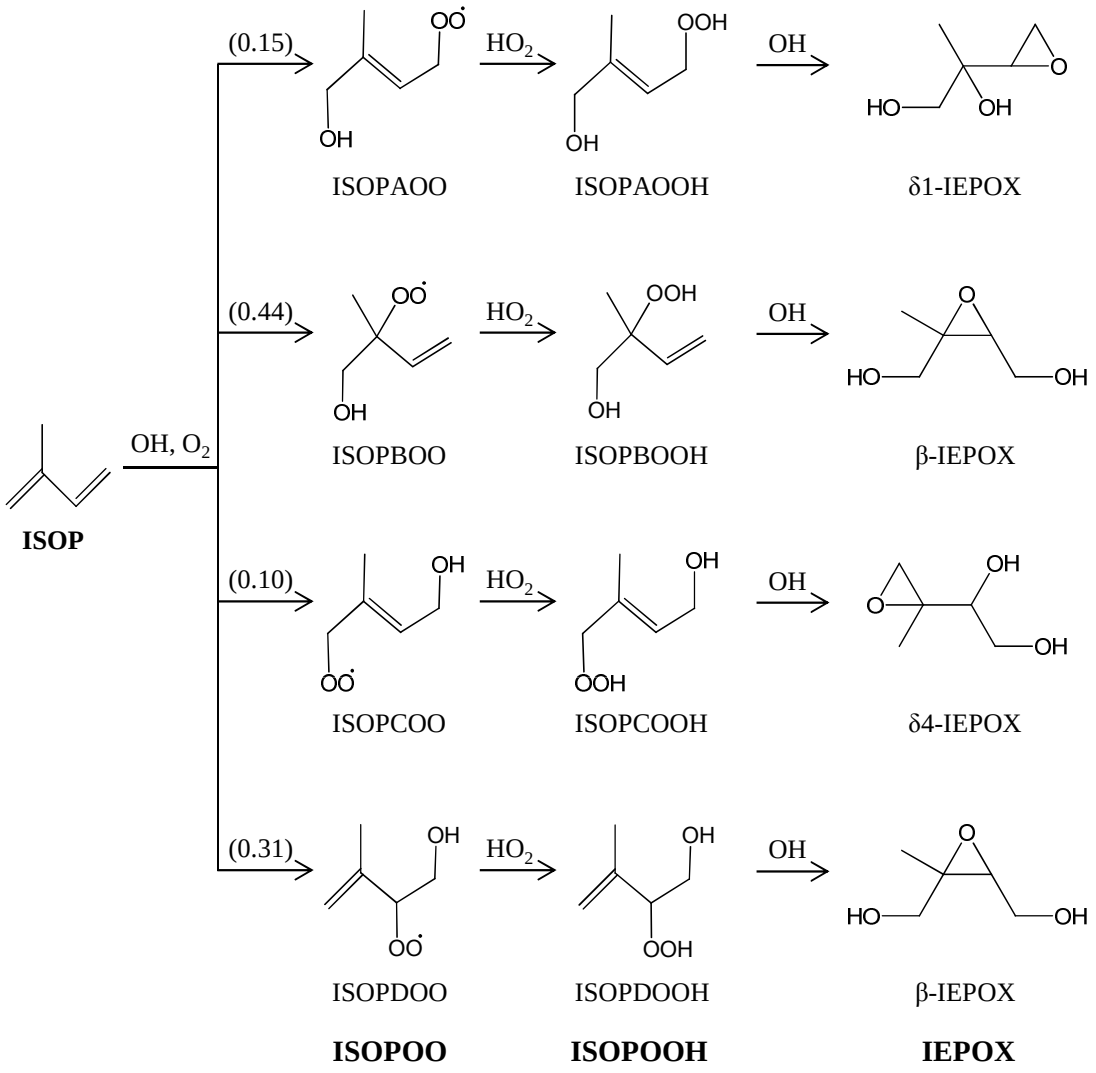
(0.15)
HO2
OH
ISOPAOO
ISOPAOOH
δ1-IEPOX
(0.44)
HO2
OH
ISOPBOO
ISOPBOOH
β-IEPOX
OH, O2
ISOP
(0.10)
HO2
OH
ISOPCOO
ISOPCOOH
δ4-IEPOX
(0.31)
HO2
OH
ISOPDOO
ISOPDOOH
β-IEPOX
ISOPOO
ISOPOOH
IEPOX

Figure S2

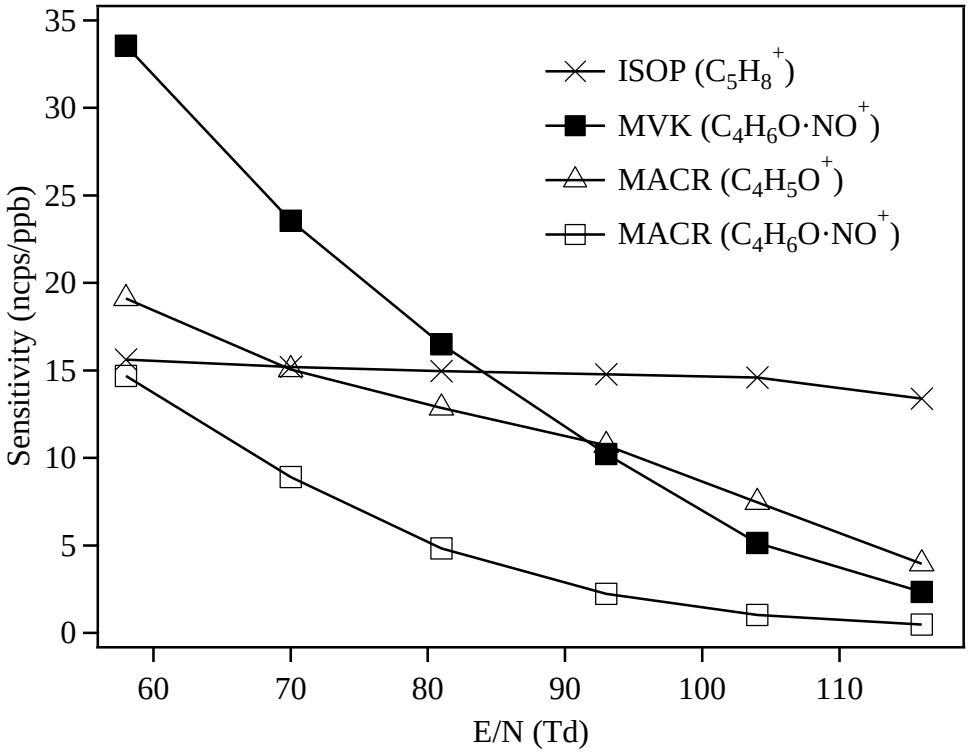
Sensitivity (ncps/ppb)
E/N (Td)
ISOP ($C_5H_8^+$)
MVK ($C_4H_6O \cdot NO^+$)
MACR ($C_4H_5O^+$)
MACR ($C_4H_6O \cdot NO^+$)
0
5
10
15
20
25
30
35
60
70
80
90
100
110

Figure S3

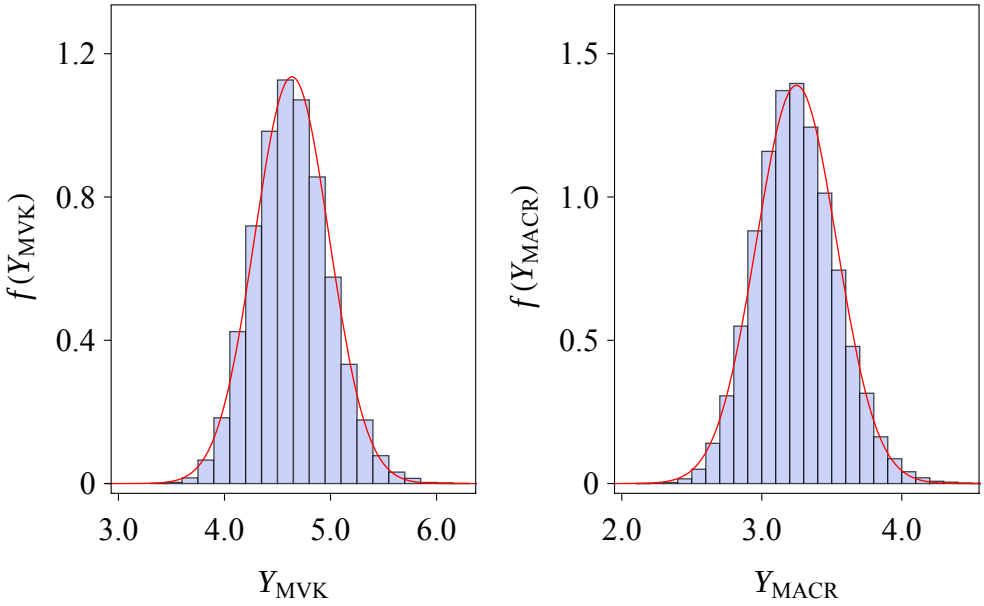

Figure S4

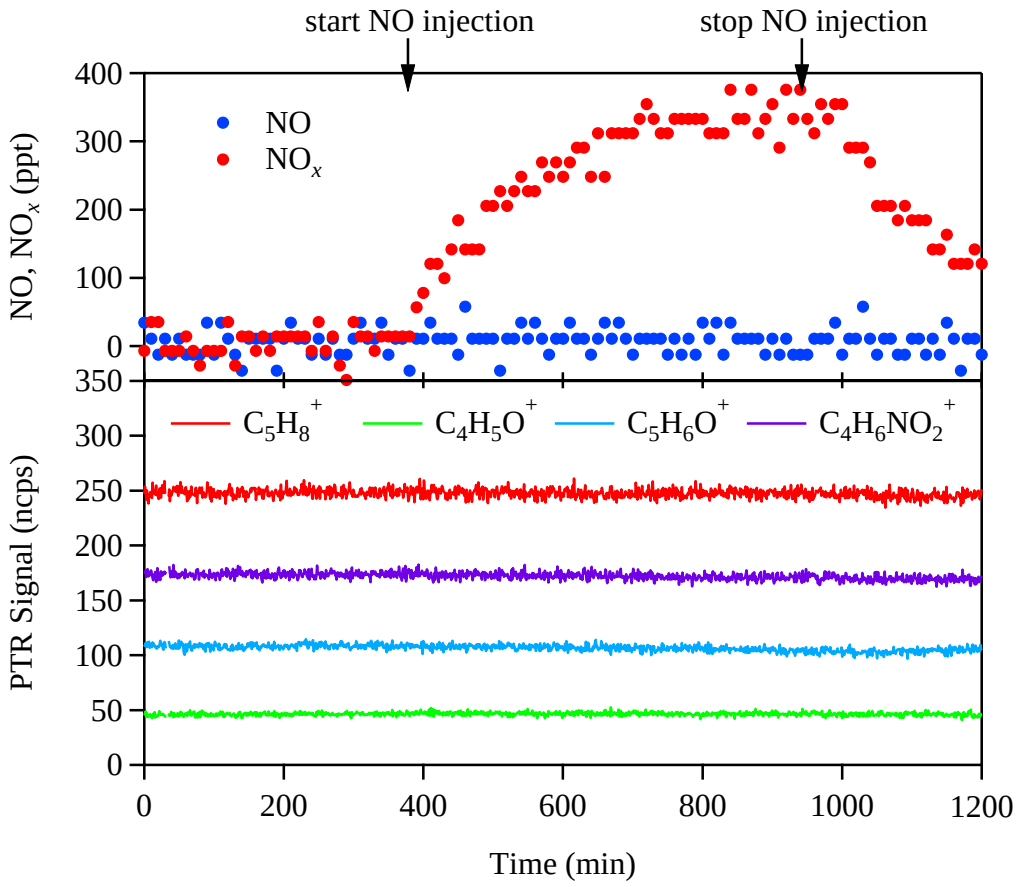
start NO injection
stop NO injection
NO
NO$_x$
NO, NO$_x$ (ppt)
400
300
200
100
0
C$_5$H$_8$$^+$
C$_4$H$_5$O$^+$
C$_5$H$_6$O$^+$
C$_4$H$_6$NO$_2$$^+$
PTR Signal (ncps)
350
300
250
200
150
100
50
0
0
200
400
600
800
1000
1200
Time (min)

Figure S5

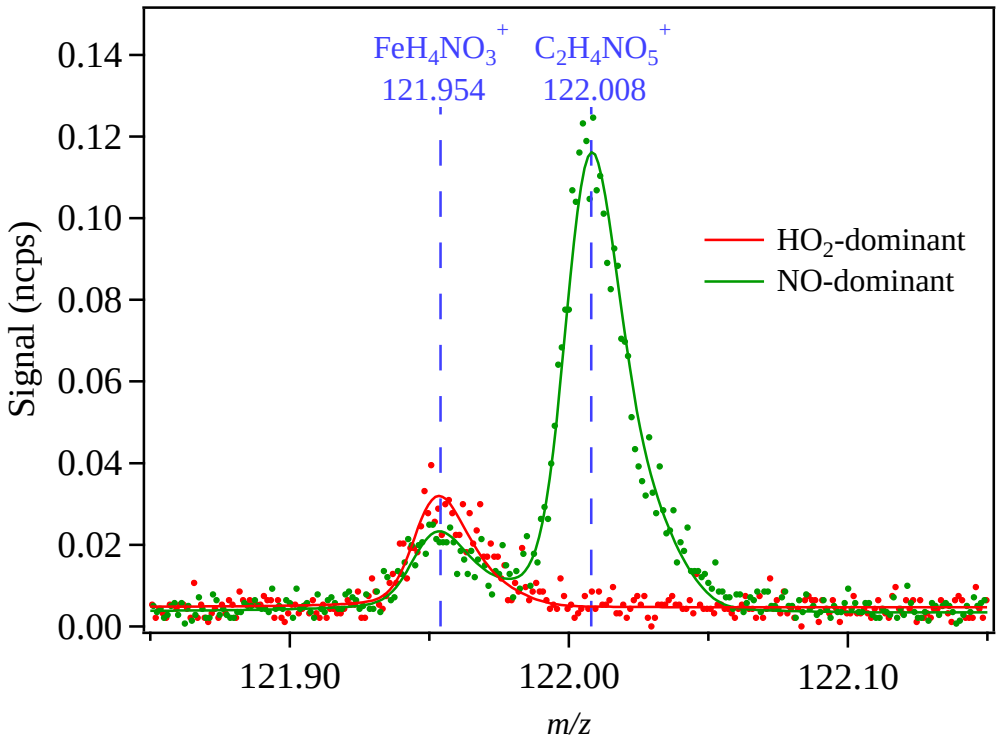
FeH4NO3+
121.954
C2H4NO5+
122.008
HO2-dominant
NO-dominant
Signal (ncps)
0.14
0.12
0.10
0.08
0.06
0.04
0.02
0.00
121.90
122.00
122.10
m/z

Figure S6

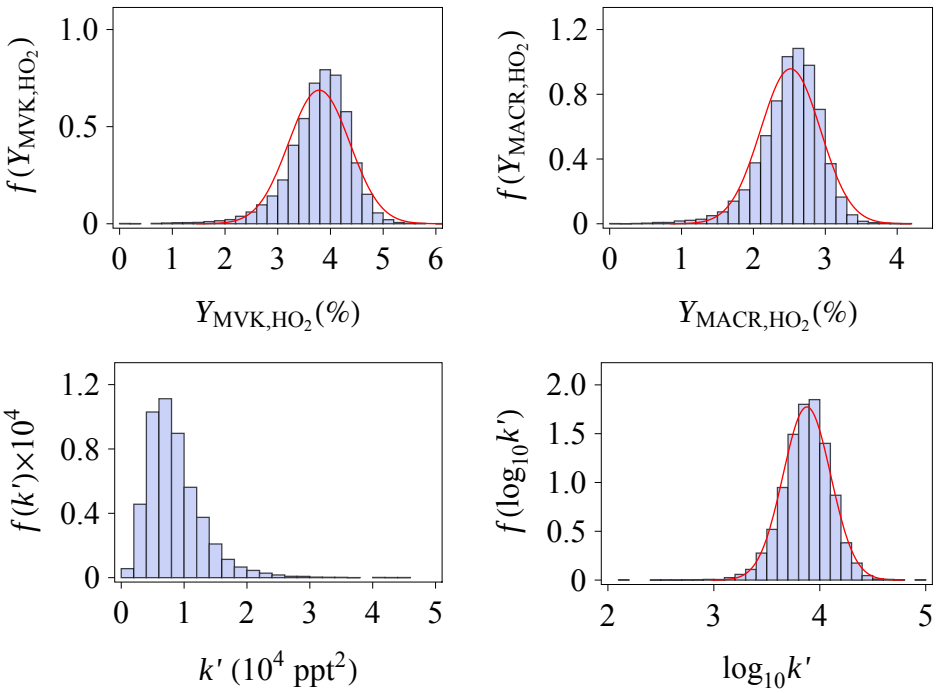
$f(Y_{MVK,HO_2})$
Y_{MVK,HO_2}(%)
$f(Y_{MACR,HO_2})$
Y_{MACR,HO_2}(%)
$f(k')\times10^4$
k' (10^4 ppt^2)
$f(\log_{10}k')$
$\log_{10}k'$

Figure S7

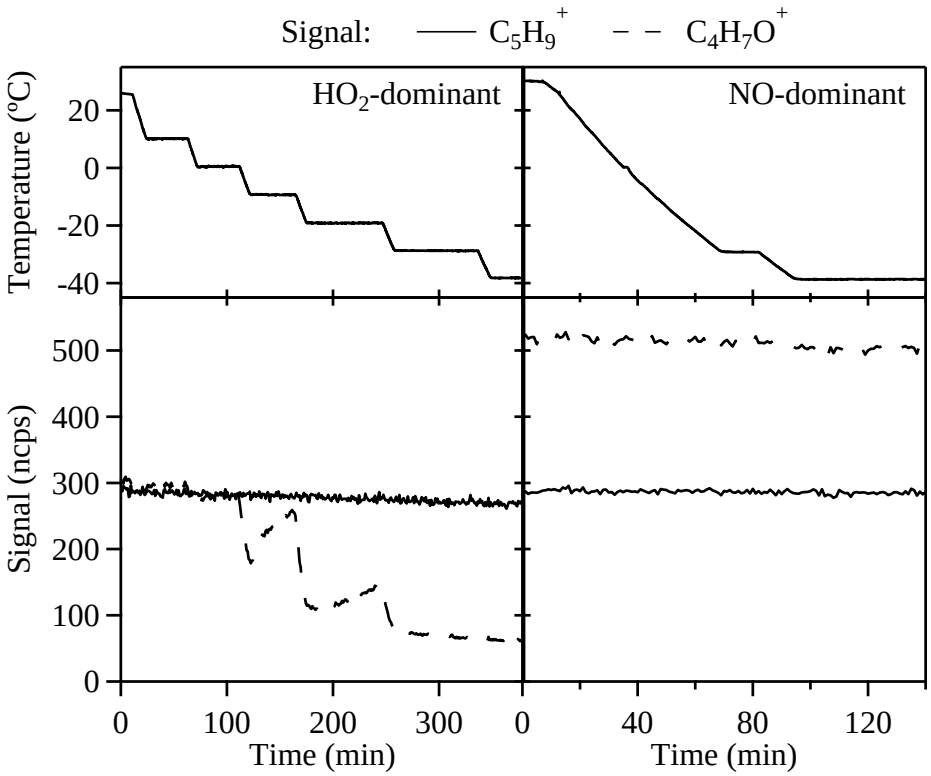
Signal: —— $C_5H_9^+$ – – $C_4H_7O^+$
HO_2-dominant
NO-dominant
Temperature (ºC)
20
0
-20
-40
Signal (ncps)
500
400
300
200
100
0
0
100
200
300
0
40
80
120
Time (min)
Time (min)

Figure S8

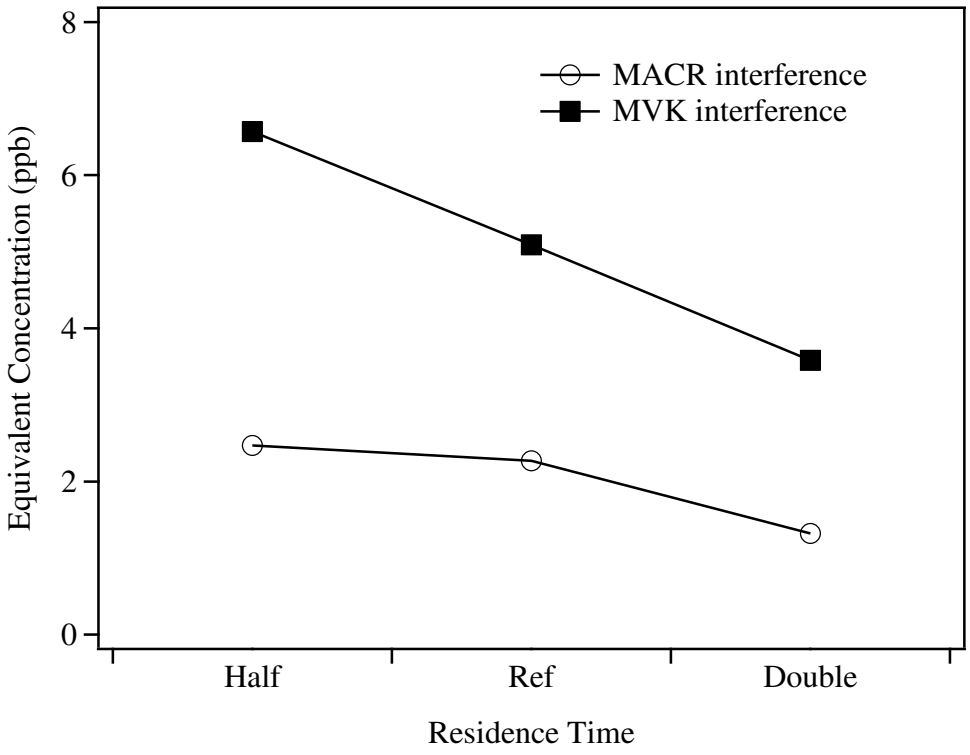
8
6
4
2
0
Equivalent Concentration (ppb)
MACR interference
MVK interference
Half
Ref
Double
Residence Time

Figure S9

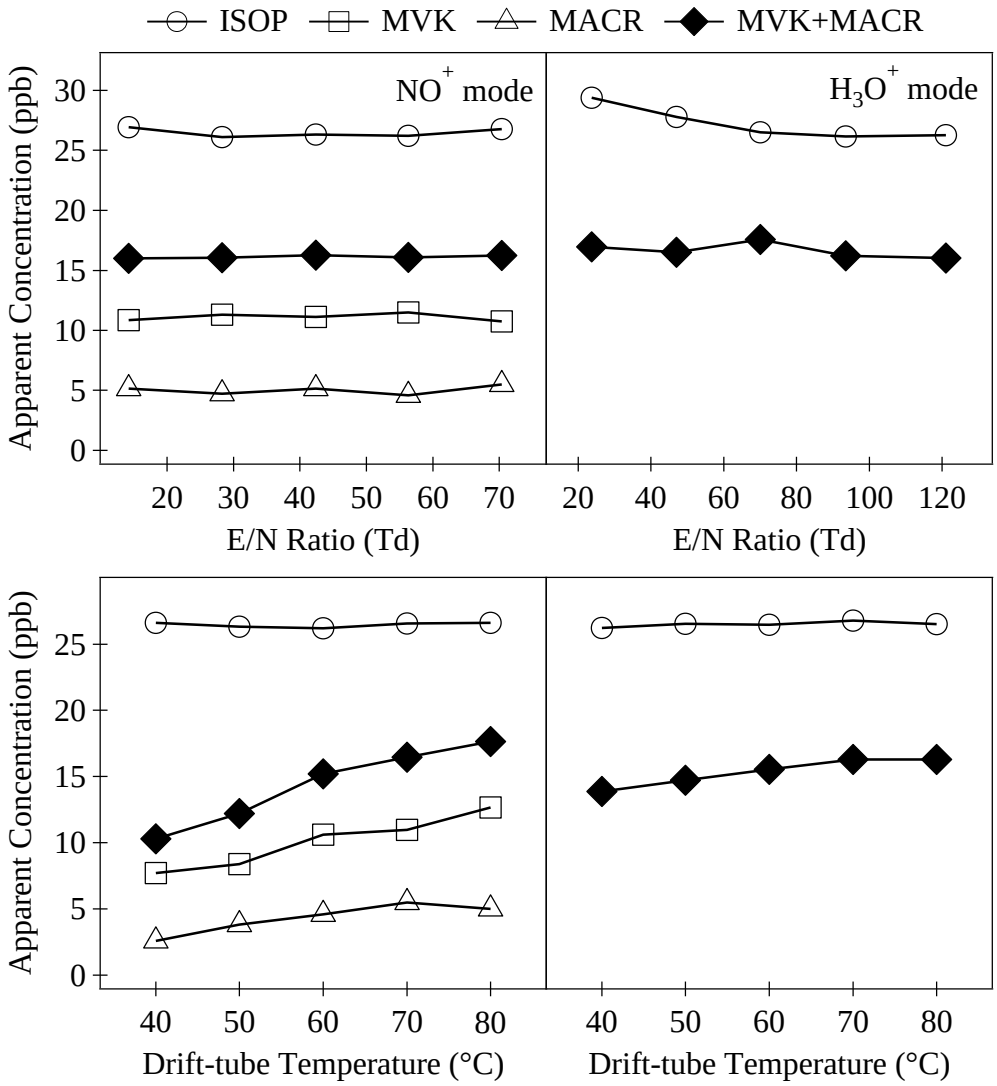
ISOP
MVK
MACR
MVK+MACR
NO+ mode
H3O+ mode
Apparent Concentration (ppb)
E/N Ratio (Td)
Drift-tube Temperature (°C)

Figure S10